Experiments in Fluids 9, 273–284 (1990)

Experiments in Fluids

Some measurements in a binary gas jet

R. M. C. So and **J. Y. Zhu** *

Mechanical and Aerospace Engineering, Arizona State University, Tempe, AZ 85287, USA

M. V. Ötügen

Aerospace Engineering Dept., Polytechnic University, Farmingdale, NY 11735, USA

B. C. Hwang

David Taylor Research and Development Centre, Annapolis, MD 21402, USA

Abstract. Simultaneous measurements of species volume concentration and velocities in a helium/air binary gas jet with a jet Reynolds number of 4,300 and a jet-to-ambient fluid density ratio of 0.64 were carried out using a laser/hot-wire technique. From the measurements, the turbulent axial and radial mass fluxes were evaluated together with the means, variances and spatial gradients of the mixture density and velocity. In the jet near field (up to ten diameters downstream of the jet exit), detailed measurements of $\overline{\varrho' u'}/\bar{\varrho}_0 \bar{U}_0$, $\overline{\varrho' v'}/\bar{\varrho}_0 \bar{U}_0$, $\bar{\varrho}\,\overline{u' v'}/\bar{\varrho}_0 \bar{U}_0^2$, $\overline{\varrho' u'^2}/\bar{\varrho}_0 \bar{U}_0^2$ and $\overline{\varrho' v'^2}/\bar{\varrho}_0 \bar{U}_0^2$ reveal that the first three terms are of the same order of magnitude, while the last two are at least one order of magnitude smaller than the first three. Therefore, the binary gas jet in the near field cannot be approximated by a set of Reynolds-averaged boundary-layer equations. Both the mean and turbulent velocity and density fields achieve self-preservation around 24 diameters. Jet growth and centerline decay measurements are consistent with existing data on binary gas jets and the growth rate of the velocity field is slightly slower than that of the scalar field. Finally, the turbulent axial mass flux is found to follow gradient diffusion relation near the center of the jet, but the relation is not valid in other regions where the flow is intermittent.

List of symbols

$a_u, a_\varrho, a_\theta, a_c$	constants in hyperbolic decay laws
c	instantaneous helium volume concentration
c'	fluctuating part of c
$\bar{C}$	mean of c
d_ε	effective jet diameter, $\sigma_1^{1/2} D$
D	jet nozzle diameter
D_{Tu}	turbulent diffusivity along x
D_{Tv}	turbulent diffusivity along r
$k_u, k_\varrho, k_\theta, k_c$	hyperbolic decay constants for u, ϱ, θ and c, respectively
N	number of samples in each data record
P	mean static pressure
r	radial coordinate measured from jet centerline
Re	jet Reynolds number, $U_j D/\nu_j$
u_i	instantaneous i^{th} component of velocity
u_i'	fluctuating part of u_i
u_i''	fluctuating part of Favre decomposition of u_i
$\bar{U}_i$	mean of u_i
$\tilde{U}_i$	Favre-averaged of u_i
u	instantaneous axial velocity
u'	fluctuating part of u
u''	fluctuating part of Favre decomposition of u
$\bar{U}$	mean of u
$\tilde{U}$	Favre-averaged of u
v	instantaneous radial velocity
v'	fluctuating part of v
v''	fluctuating part of Favre decomposition of v
$\bar{V}$	mean of v
$\tilde{V}$	Favre-averaged of v
x	axial coordinate measured from jet nozzle exit
x_i	i^{th} component of coordinates
x_0	virtual origin of jet

Greek symbols

α	density ratio parameter, $(\varrho_h/\varrho_a - 1)$
δ_c	jet half width based on $\bar{C}$ profile
δ_u	jet half width based on $\bar{U}$ profile
δ_u'	jet width based on $\bar{U}/\bar{U}_0 = 0.75$
δ_θ	jet half width based on $\bar{\theta}$ profile
η	dimensionless r-coordinate, r/δ_u
η_θ	dimensionless r-coordinate, r/δ_θ
θ	instantaneous mixture mass fraction or temperature
θ'	fluctuating part of θ
$\bar{\theta}$	mean of θ
ϱ	instantaneous mixture density
ϱ'	fluctuating part of ϱ
$\bar{\varrho}$	mean of ϱ
σ_1	density ratio of jet, ϱ_j/ϱ_a
μ_T	turbulent viscosity
ν	fluid kinematic viscosity

Subscripts

a	air
h	helium
j	jet
o	centerline values

Overscores

$-$	time-averaged value
$\sim$	Favre-averaged value

1 Introduction

The simultaneous measurements of density and velocity in an isothermal, variable-density flow were first attempted by

* Present address: Mechanical Engineering Dept., University of California, Irvine, CA 92717, USA

Stanford and Libby (1974) using the hot-wire probe developed by Way and Libby (1970). Based on these measurements, they demonstrated that some of the turbulent mass flux terms normally neglected in the jet equations were not small. Their study was carried out primarily to demonstrate the validity and viability of the hot-wire probe, therefore, detailed measurements of the jet mixing process were not attempted.

Because of the elaborate calibration process involved, the hot-wire probe is not very convenient to use. An alternative technique using Rayleigh scattering to measure concentration and hot-wire to measure velocity was suggested by Pitts et al. (1983). Even then, the velocity measurements were very sensitive to species concentration and to the hot-wire calibration constants. Recent applications of optical techniques to measure concentration in non-reacting flows have been reviewed by Gouldin et al. (1986). For example, Batt (1977) suggested the use of fiber-optic probes for the measurement of $N\,O_x$ concentration, while Raman and Rayleigh scattering techniques were successfully used to measure methane concentration in free jets by Birch et al. (1978) and by Pitts and Kashiwagi (1984), respectively, and Coherent Anti-Stokes Raman Spectroscopy (CARS) technique was applied to measure temperature by Fujii et al. (1983). These techniques were superior to the hot-wire probe because the concentration measurements were independent of velocity.

On the other hand, laser Doppler anemometer (LDA) is capable of resolving the velocity field independent of the scalar field, therefore, it can be combined with other optical techniques to measure the velocity and scalar fields simultaneously. Even though simultaneous LDA/Raman, LDA/Rayleigh and LDA/CARS techniques have been used to study premixed (Moss 1980; Fujii et al. 1984; Goss et al. 1988) and non-premixed (Driscoll et al. 1982; Dibble et al. 1984) flames, they have not been used to study the behaviour of $\bar{\varrho}\,\overline{u_i' u_j'}$, $\overline{\varrho' u_i'}$ and $\overline{\varrho' u_i' u_j'}$ in detail, either in jet flames or in non-reacting binary gas jets. Nevertheless, the flame studies led to an understanding of mass transfer in reacting flows and showed that, because of heat release effects, the gradient diffusion assumption that was commonly made to model turbulent axial mass flux in first order closure theories was not valid (Driscoll et al. 1982). In spite of these advances, the relative roles of $\overline{\varrho' u_i'}$ and $\overline{\varrho' u_i' u_j'}$ compared to $\bar{\varrho}\,\overline{u_i' u_j'}$ in isothermal, variable-density flows is still not well understood.

This is not the case in the study of heat transport. For example, in the studies of heated jets in a general stream, the correlations $\overline{u'\theta'}$, $\overline{v'\theta'}$, $\overline{u'^2\theta'}$, $\overline{v'^2\theta'}$, $\overline{u'^2 v'}$ and $\overline{u' v'^2}$ have been measured and critically analyzed (Antonia et al. 1975; Chevray and Tutu 1978). In these studies, the temperature difference between the jet and the surrounding fluid was purposely maintained low so that temperature could be treated as a dynamically passive scalar and the density field was essentially constant. As a result, hot-wire techniques could be used to measure the instantaneous u and v simultaneously with the instantaneous temperature. Unfortunately, up to now, similar studies of mass transport are not available, in spite of the tremendous advance made in the development of various optical and scattering techniques (Gouldin et al. 1986).

Recently, Zhu et al. (1988) used a LDA to measure velocity and a hot-wire type concentration probe (Brown and Roshko 1974) to measure helium volume concentration simultaneously in an axisymmetric sudden-expansion flow. Since the concentration probe of Brown and Roshko (1974) measured species volume concentration independent of the upstream velocity and the LDA measured velocity independent of species concentration, the resultant concentration and velocity measurements were free of each other's influence. Zhu et al. (1989) subsequently used the laser/hot-wire technique to measure $\overline{\varrho' u'}$ and $\overline{\varrho' v'}$ in the near field of a helium/air mixture free jet. Their studies demonstrate that the laser/hot-wire technique is a viable alternative to LDA/Raman or LDA/Rayleigh techniques in the study of isothermal, variable-density mixing. Therefore, the present investigation proposes to use the laser/hot-wire technique to study in detail the turbulent mass transport behavior in a helium/air jet.

The objectives of the present study are to attempt to measure $\overline{\varrho' u'}$, $\overline{\varrho' v'}$, $\overline{\varrho' u'^2}$, $\overline{\varrho' v'^2}$ and $\bar{\varrho}\,\overline{u' v'}$ in a binary gas jet and to use the results to assess the significance of these terms in the governing jet equations. An attempt is also made to evaluate the difference between Favre- and Reynolds-averaged velocity in the binary gas jet investigated. The laser/hot-wire technique of Zhu et al. (1988) is used to measure the jet characteristics and the results are compared with literature data. Thus, the validity and viability of the laser/hot-wire technique can be further verified. The jet measurements are used to study jet growth and decay laws. Furthermore, the concept of an effective diameter (Thring and Newby 1953) is used to test the universality of the decay laws.

2 Experimental setup and measurement technique

A schematic of the test rig, arranged vertically, is shown in Fig. 1. Here, the jet near field is assumed to cover the region, $0 \leq x/D \leq 10$. Downstream of this region is referred to as the jet far field. The dimensions of the various components are as labelled and the schematic shown is not drawn to scale. Helium and air were premixed to the correct proportion by volume and the mixture was delivered to the jet nozzle plenum. The mixture supply pressure was carefully regulated by a pressure gauge (not shown in Fig. 1) and, once the jet condition was set, the gauge reading was maintained constant throughout the experiment. The flow was properly conditioned by a honeycomb section in the plenum, followed by a well-contoured convergent nozzle (designed to ASME specifications). Consequently, the flow exiting the nozzle had a low turbulence level and the velocity and mixture mass fraction were quite uniform across the nozzle. The jet velocity was set approximately to 11.6 m/s and σ_1 was chosen to

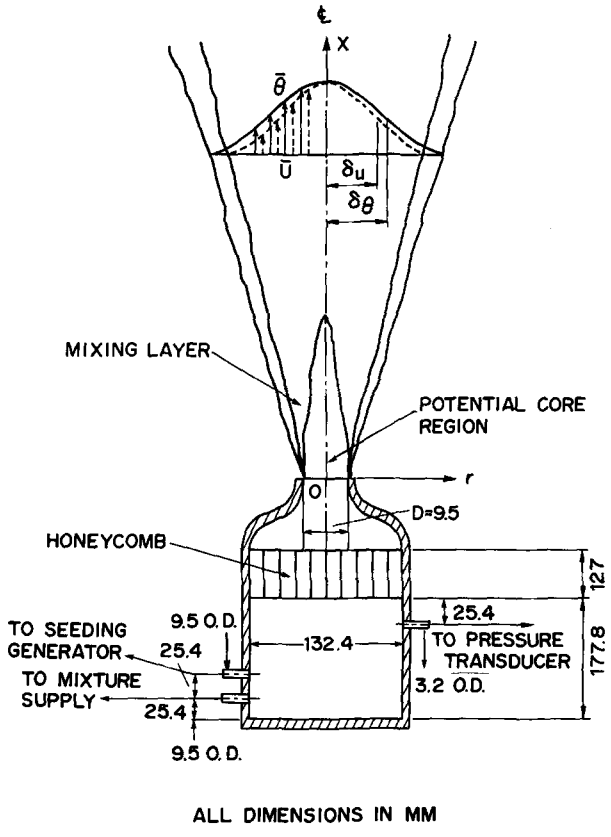

Fig. 1. Schematic of test rig

be 0.64. This gave a Reynolds number of 4,300 and a Richardson number of 1.5×10^{-2} at the nozzle exit plane. Therefore, buoyancy effects became important only at $\sim 45\ D$ downstream of the nozzle.

Basically, the laser/hot-wire technique consisted of a one-component laser Doppler anemometer (LDA) and a hot-wire type concentration probe (see So et al. 1987 for details of the equipment). A block diagram showing the arrangement of the various equipment is given in Fig. 2. The concentration probe was calibrated to measure helium volume concentration alone and was independent of the approach flow velocity. So and Ahmed (1987) and So et al. (1987) have also used the probe to make measurements in a swirling and a rotating flow and found that the probe response was unaffected by the rotating velocity field. The concentration probe had a capture volume of ~ 0.4 mm in diameter. It was positioned slightly above and behind the laser beam measuring volume. The arrangement gave a combined measuring volume of about 1 mm in diameter (Zhu et al. 1988); thus, the spatial resolution of the laser/hot-wire technique is slightly better than the LDA/Rayleigh scattering technique of Driscoll et al. (1982).

The effect of the probe's presence on the LDA measurements and the influence of seeding particles on the hot-wire response have been thoroughly examined by Zhu et al. (1988) and were found to be negligible. Therefore, the technique is both accurate and reliable when used to measure velocity and concentration simultaneously. Concentration

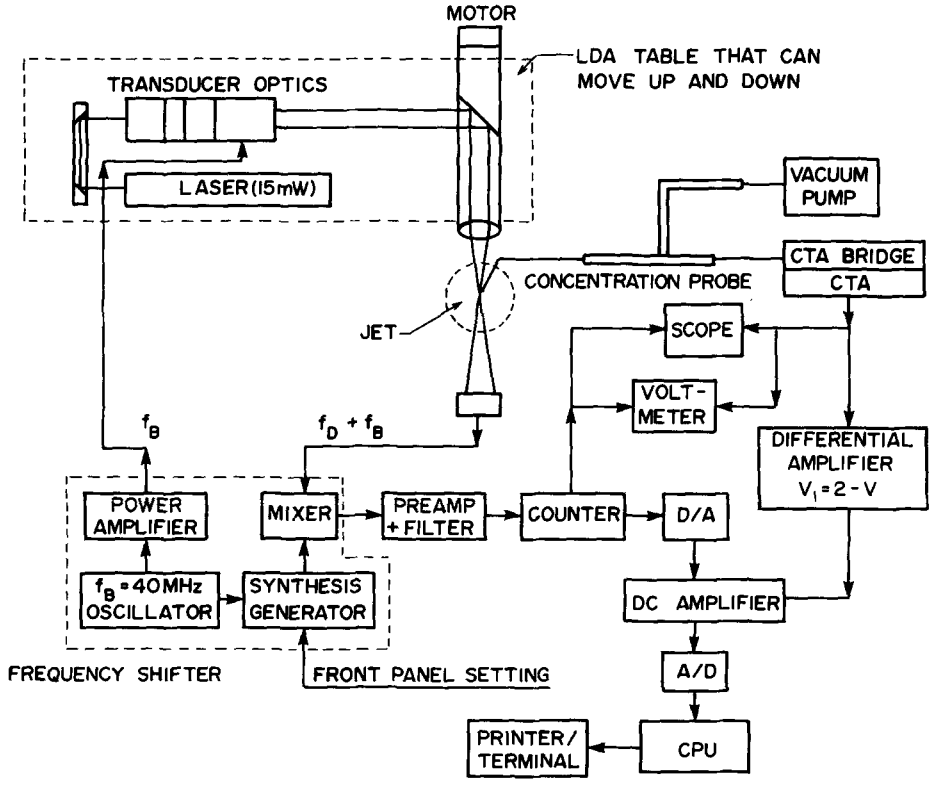

Fig. 2. Block diagram of laser/hot-wire technique

and axial velocity were measured first, then the laser optics were rotated by $\pi/2$ to measure the radial velocity and concentration simultaneously. Since ϱ and θ are related to c by

$$\varrho = \varrho_a(1-c) + \varrho_h c, \tag{1}$$

and

$$\theta = \frac{(1+\alpha)\,c}{1+\alpha\,c}, \tag{2}$$

the signals for ϱ and θ are easily constructed once c is known. Therefore, the statistics of ϱ and θ and hence the correlations $\overline{\varrho' u'}$, $\overline{\varrho' v'}$, $\overline{\varrho' u'^2}$, $\overline{\varrho' v'^2}$ etc. can be evaluated without approximations.

The present study concentrates on understanding the time-averaged structure of the binary gas jet and attempts to provide information on turbulent properties and growth and decay behavior, which may be used to develop improved computational models for the stationary analysis of such flows. Therefore, unconditional sampling was used to measure velocity and helium volume concentration. Digital LDA information was first converted to analog signal using a commercial D/A converter and subsequently digitized together with the hot-wire signal at constant intervals. The air surrounding the jet contained sufficient dust and artificial seed particles to generate a relatively good LDA signal. Thus, individual samples contributed information on the mean jet, irrespective of the occasional presence of the surrounding fluid within the probe, especially near the jet edge where the flow is expected to be intermittent. This prevented measurements from being "conditional". However, the jet fluid had a higher particle concentration than the ambient and beyond $x/D=10$, a decrease in the LDA signal rate was observed. Near the jet edge, small entrainment velocity further reduced the LDA data validation rates, especially in attempts to measure v. As a result, the simultaneous measurements of ϱ and v beyond $x/D=10$ were deemed unreliable and, therefore, were not attempted in this study. The measurements obtained in the region $0 \le x/D \le 10$ include the individual statistics of ϱ, u and v and the correlations $\overline{\varrho' u'}$, $\overline{\varrho' v'}$, $\overline{\varrho' u'^2}$ and $\overline{\varrho' v'^2}$, as well as the Reynolds shear stress, $\bar{\varrho}\,\overline{u' v'}$. Beyond $x/D=10$, only the correlations $\overline{\varrho' u'}$ and $\overline{\varrho' u'^2}$ are available. With a one-component LDA system, the Reynolds shear stress $\bar{\varrho}\,\overline{u' v'}$ had to be derived using the method described by Logan (1972). This was accomplished by rotating the laser optics by $\pm\pi/4$ about the jet axis and making additional measurements.

The sampling rate was always chosen to be much less (roughly an order of magnitude) than the particle arrival rate in order to avoid bias in the velocity measurements (Stevenson et al. 1982). Consequently, the velocity data were sampled at fairly low rates and spectral calculations were not attempted. However, the single and joint probability density distributions and statistical calculations were not affected by the low sampling rate. This paper discusses only the basic statistics of the binary jet. A more penetrating analysis of the single and joint probability density distributions and the higher-order statistics will be presented in a later report.

Several simple experiments were carried out to study the effect of record length on the calculated statistics. The results showed that all calculated statistics settle to a constant value for sampling sizes of $N \ge 10{,}000$. Therefore, a 24,000 sample record used to analyze all signals was judged to be sufficient to guarantee that all calculated quantities were independent of record length and unbiased.

3 Qualification experiment

The measurements at $x/D=0.46$ across the jet have been reported by Zhu et al. (1989). They showed that $\bar{U}$ and $\bar{\theta}$ were uniform over 90% of D and were symmetric about the jet centerline. Furthermore, $\overline{u'^2}/\bar{U}_0^2 \simeq 1.4\times10^{-4}$ and $\overline{\theta'^2}/\bar{\theta}_0^2 \simeq 1.4\times10^{-4}$ and were uniform over 80% of D. On the other hand, $\overline{\varrho' u'}$ and $\overline{\varrho' v'}$ were not uniform across the jet but their values were small, with $-\overline{\varrho' u'}/\bar{\varrho}_0\,\bar{U}_0$ varying from zero to 1.2×10^{-5} in the same region. Again, the mass flux quantities were symmetric about the jet centerline. The present measurements are identical to those reported by Zhu et al. (1989). Therefore, the jet exit conditions are axisymmetric, uniform and the turbulence level is low.

The integrity of the jet far downstream was examined by measuring both u and c across the jet. A typical measurement at $x/D=24.46$ is shown in Fig. 3. Here, the measurements of $\bar{U}/\bar{U}_0$, $\bar{\theta}/\bar{\theta}_0$, $\sqrt{\overline{u'^2}}/\bar{U}_0$ and $\sqrt{\overline{\theta'^2}}/\bar{\theta}_0$ are shown plotted against r/δ_u for the velocity data and against r/δ_θ for the mixture mass fraction data. The profiles are symmetric to within experimental measurement errors. Consequently, the present facility provides an axisymmetric, free binary gas jet for investigation.

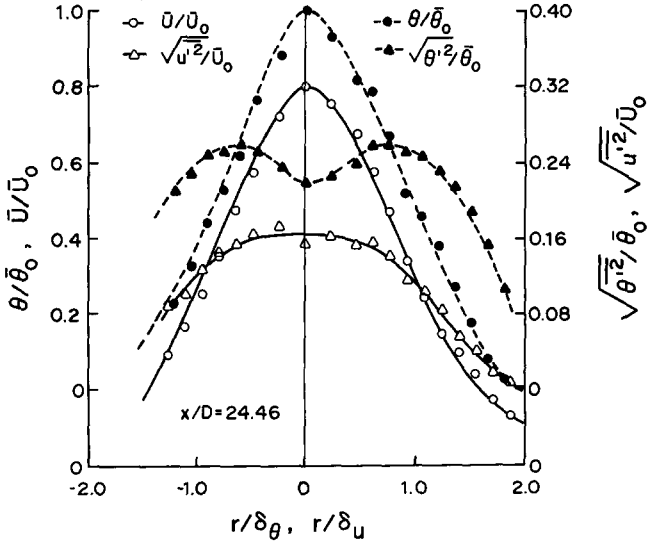

Fig. 3. Symmetry check on binary gas jet

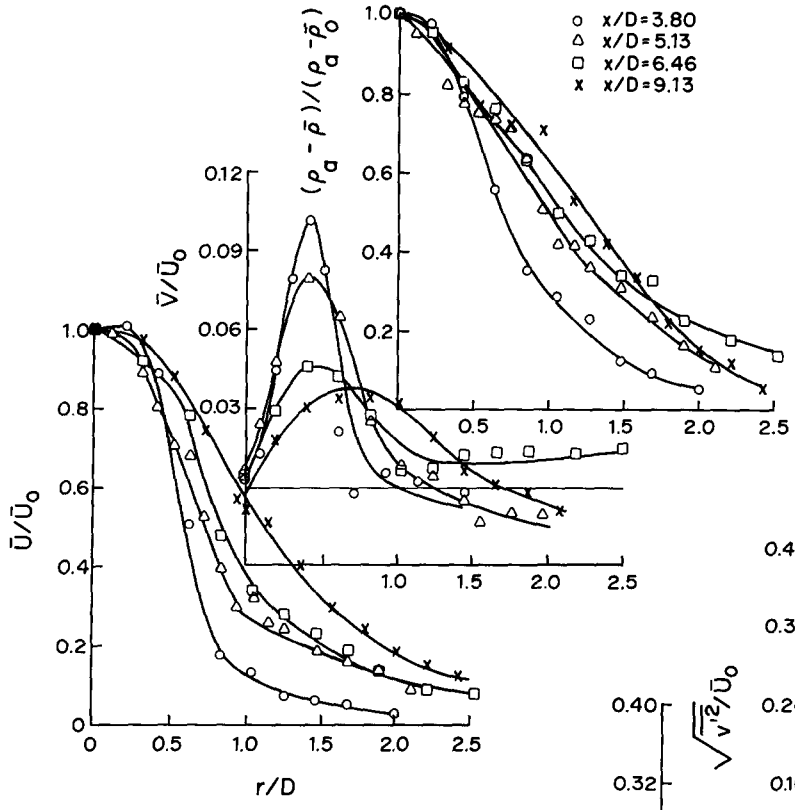

Fig. 4. Mean jet properties in the near field

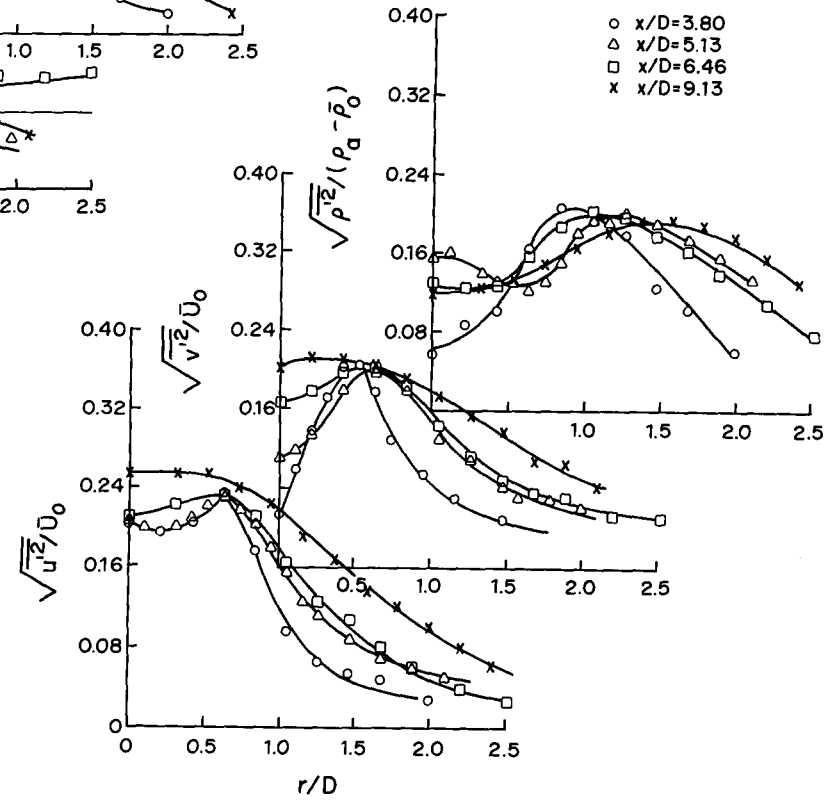

Fig. 5. Jet turbulence properties in the near field

4 Near field behavior

In the jet near field ($0 \leq x/D \leq 10$), measurements of u, v and c were carried out at the following locations: $x/D = 3.80$, 5.13, 6.46 and 9.13 according to the procedures described in Sect. 2. Furthermore, $\overline{u'v'}$ was also measured using the $\pm\pi/4$ technique and without the presence of the concentration probe. The mean velocities obtained from this measurement were found to be in excellent agreement with those obtained by simultaneously measuring ϱ and u or ϱ and v. This again serves to verify that the presence of the concentration probe does not adversely affect the velocity measurements.

It is obvious that the jet is still developing even at $x/D = 9.13$ (Figs. 4 and 5). However, the approach to a Gaussian error function distribution for $\bar{U}/\bar{U}_0$ and $(\varrho_a - \bar{\varrho})/(\varrho_a - \varrho_0)$ is clearly indicated by the data (Fig. 4). The radial velocity in the region, $0 < x/D < 6.46$, seems high compared to the far field air jet measurements of Wygnanski and Fiedler (1969). However, at $x/D = 9.13$, $\bar{V}/\bar{U}_0$ quickly settles to a much lower value consistent with the air jet measurements. As expected, the radial velocity in the outer region of the jet is negative. The variance of u, v and ϱ, normalized by their respective centerline values, show a peak away from the jet centerline in the region $0 < x/D < 9.13$ (Fig. 5). The locations of the peaks for $\overline{u'^2}$ and $\overline{v'^2}$ seem to coincide. Their occurrence is a direct consequence of the formation of an axisymmetric mixing layer just outside of the velocity potential core region of the jet (Fig. 1). The maximum mixing activity moves towards the jet centerline as x/D increases. The same is not true of the density field since the peak in $\overline{\varrho'^2}$ is still located away from the jet centerline at $x/D = 9.13$ (Fig. 5).

The flux terms, $\bar{\varrho}\,\overline{u'v'}$, $\overline{\varrho' u'}$ and $\overline{\varrho' v'}$ are plotted in Fig. 6, while the triple correlations, $\overline{\varrho' u'^2}$ and $\overline{\varrho' v'^2}$, are shown in

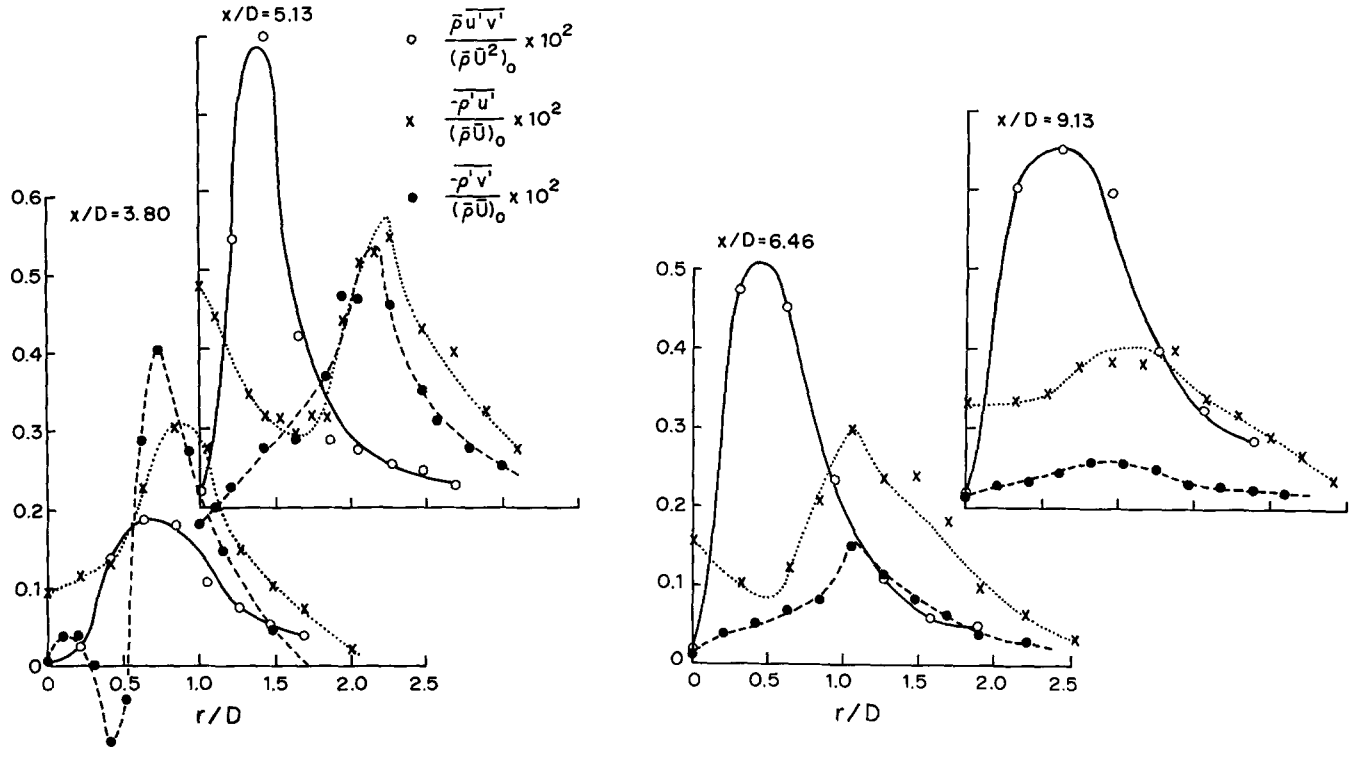

Fig. 6. Behavior of momentum and mass fluxes across the jet

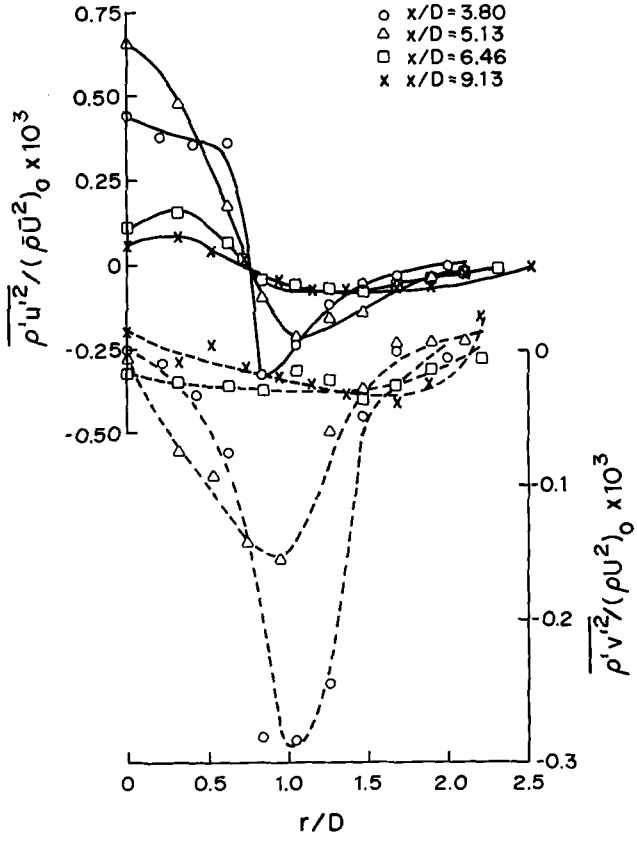

Fig. 7. Distributions of triple correlations across the jet

Fig. 7. Again, the measurements are normalized by the respective centerline values. At $x/D=3.80$, the Reynolds shear stress is smaller than the mass fluxes (Fig. 6). Its maximum occurs at a smaller r/D than the locations of the maximum for $\overline{\varrho' u'}$ and $\overline{\varrho' v'}$. However, $\bar{\varrho}\,\overline{u' v'}$ quickly develops and becomes significantly larger than $\overline{\varrho' v'}$ at $x/D=9.13$. The locations where the maximum of $\overline{\varrho' u'}$ and $\overline{\varrho' v'}$ occur move slightly away from the jet centerline in the downstream direction and become coincident at $x/D=5.13$. Interestingly, the r/D value for maximum $\bar{\varrho}\,\overline{u' v'}$ is always smaller than the corresponding values for $\overline{\varrho' u'}$ and $\overline{\varrho' v'}$. As expected, $\bar{\varrho}\,\overline{u' v'}$ and $\overline{\varrho' v'}$ approach zero at the jet centerline, a condition dictated by jet symmetry. The decay of $\overline{\varrho' u'}$ is much slower than that of $\overline{\varrho' v'}$. Initially, they measure about the same across the jet, except near the jet core. However, by $x/D=9.13$, $\overline{\varrho' v'}/\overline{\varrho' u'}$ is about 0.25 across the jet, thus, indicating that the dilution of the initial jet is through turbulent transport mostly in the axial direction rather than the radial direction.

The rate of change of all these quantities with respect to x is approximately the same, but the rate of change with respect to r is largest for $\bar{\varrho}\,\overline{u' v'}$. In the region, $0 \le x/D \le 6.46$, the radial gradient of all three fluxes are of the same order of magnitude, but at $x/D=9.13$, $\partial(\bar{\varrho}\,\overline{u' v'})/\partial r$ is at least one order of magnitude larger than $\partial/\partial r$ of $\overline{\varrho' u'}$ and $\overline{\varrho' v'}$. The triple correlations are at least one order of magnitude smaller than the mass fluxes (Fig. 7). Even though the present experiment does not provide measurement of $\overline{\varrho' u' v'}$, judging from the values of $\overline{\varrho' u'^2}$ and $\overline{\varrho' v'^2}$, it can be inferred

that the normalized $\overline{\varrho' u' v'}$ is also one order of magnitude smaller than similarly normalized $\overline{\varrho' u'}$ and $\overline{\varrho' v'}$.

If the gradient diffusion assumption is invoked for the momentum and mass fluxes, then

$$-\bar{\varrho}\,\overline{u' v'} = \mu_T \frac{\partial \bar{U}}{\partial r}, \tag{3}$$

$$-\overline{\varrho' u'} = D_{Tu} \frac{\partial \bar{\varrho}}{\partial x}, \tag{4}$$

$$-\overline{\varrho' v'} = D_{Tv} \frac{\partial \bar{\varrho}}{\partial r}. \tag{5}$$

Since the turbulence field is non-isotropic except for a small region around the jet axis, the values of D_{Tu} and D_{Tv} cannot be assumed equal. Furthermore, the turbulent viscosity and diffusivities can also be varying with x and r. In spite of these characteristics, a way to test the appropriateness of these relations can still be achieved by plotting the fluxes versus the respective mean gradients. If the fluxes $\bar{\varrho}\,\overline{u' v'}$, $\overline{\varrho' u'}$ and $\overline{\varrho' v'}$ are of opposite sign to their respective mean gradients, then it can be said that (3)–(5) are appropriate. However, μ_T, D_{Tu} and D_{Tv} do not have to be constant. Zhu et al. (1989) have examined (4) and (5) and found that they are appropriate for the jet core region only, where $\overline{\varrho' u'}$ and $\overline{\varrho' v'}$ are of opposite sign to $\partial\bar{\varrho}/\partial x$ and $\partial\bar{\varrho}/\partial r$, respectively. Since $\bar{\varrho}\,\overline{u' v'}$ is positive across the jet (Fig. 6) and $\partial\bar{U}/\partial r$ is negative in the same region (Fig. 4), (3) is also an appropriate relation for the momentum flux. It should be pointed out that even though the sign of the terms in (3)–(5) agrees, the respective turbulent diffusivity coefficients do vary across the jet, thus, rendering the use of these relations difficult.

If the jet Reynolds number is very high, viscous effects can be neglected, then the Reynolds equations for isothermal, binary gas jets can be written without approximations as:

$$\frac{\partial}{\partial x}[r(\bar{\varrho}\,\bar{U} + \overline{\varrho' u'})] + \frac{\partial}{\partial r}[r(\bar{\varrho}\,\bar{V} + \overline{\varrho' v'})] = 0, \tag{6}$$

$$\frac{\partial}{\partial x}(\bar{\varrho}\,\bar{U}^2) + \frac{\partial}{\partial r}(\bar{\varrho}\,\bar{U}\,\bar{V}) = -\frac{\partial P}{\partial r} - \frac{\partial}{\partial x}[2\overline{\varrho' u'}\,\bar{U} + \bar{\varrho}\,\overline{u'^2} + \overline{\varrho' u'^2}] - \frac{\partial}{\partial r}[\overline{\varrho' u'}\,\bar{V} + \overline{\varrho' v'}\,\bar{U} + \bar{\varrho}\,\overline{u' v'} + \overline{\varrho' u' v'}], \tag{7}$$

$$\frac{\partial}{\partial x}(\bar{\varrho}\,\bar{U}\,\bar{V}) + \frac{\partial}{\partial r}(\bar{\varrho}\,\bar{V}^2) = -\frac{\partial P}{\partial r} - \frac{\partial}{\partial x}[\overline{\varrho' u'}\,\bar{V} + \overline{\varrho' v'}\,\bar{U} + \bar{\varrho}\,\overline{u' v'} + \overline{\varrho' u' v'}] - \frac{\partial}{\partial r}[2\overline{\varrho' v'}\,\bar{V} + \bar{\varrho}\,\overline{v'^2} + \overline{\varrho' v'^2}]. \tag{8}$$

Conventional wisdom is to invoke the boundary-layer approximations to simplify (6)–(8). In addition, $\overline{\varrho' u' v'}$, $\overline{\varrho' u'^2}$ and $\overline{\varrho' v'^2}$ are assumed small and hence are neglected compared to $\bar{\varrho}\,\overline{u' v'}$. As a result, the governing jet equations are simplified to consist of the underlined terms only. The simplified equations may be true for the jet far field (Libby 1962; Ferri et al. 1964). However, the validity of the simplified equations for the jet near field has not been sufficiently demonstrated. The present results show that, in the jet near field, the double underlined terms in (6)–(8) cannot be neglected when compared to the underlined terms. Consequently, the resultant jet equations for the near field should also include the r-momentum equation and are different from the far field equations. On the other hand, if the equations are written in terms of the Favre-averaged variables, then all the mass flux and triple correlation terms disappear. The resultant equations are similar to those assumed for the far field (Bilger 1976). However, the question of how to model the Favre-averaged momentum flux terms still remains.

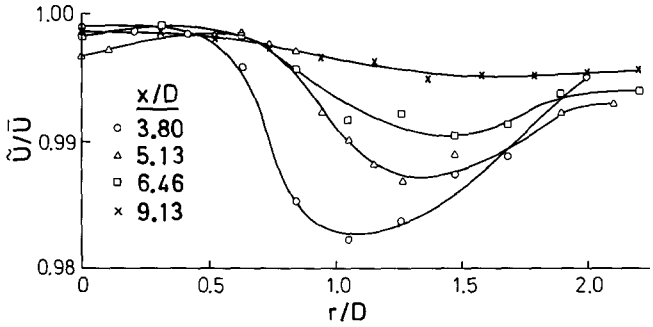

Fig. 8. Estimate of the ratio $\tilde{U}/\bar{U}$ across the jet

Assuming that the constant-density models can be extended to the Favre-averaged quantities without modifications, the question of comparison with measurements still needs to be addressed. Since $\overline{\varrho' u'}$ is measured, the ratio $\tilde{U}/\bar{U}$ can be evaluated according to $\tilde{U} = \bar{U} + \overline{\varrho' u'}/\bar{\varrho}$. The results for the near field are shown in Fig. 8. It can be seen that $\tilde{U}/\bar{U}$ is always greater than 0.98, and its value is very close to one across the jet at $x/D = 9.13$. The difference between $\tilde{U}$ and $\bar{U}$ is small for the binary gas jet investigated. On the other hand, $\tilde{V}/\bar{V} = 1 + \overline{\varrho' v'}/(\bar{\varrho}\,\bar{V})$. Since $\overline{\varrho' v'}/\overline{\varrho_0}\,\overline{U_0}$ is of order 10^{-2} (Fig. 6) and $\overline{\varrho' v'}/\bar{\varrho}_0\,\bar{U}_0$ is of order 10^{-1} (Fig. 4), the maximum value of the correction term for $\tilde{V}/\bar{V}$ is about 0.1. However, this decreases to about 0.03 at $x/D = 9.13$, which is three times larger than the corresponding correction for $\tilde{U}/\bar{U}$. Therefore, while the calculated $\tilde{U}$ can be directly compared with the measured $\bar{U}$ without having to account for the $\overline{\varrho' u'}/(\bar{\varrho}\,\bar{U})$ correction, the same is not true for $\tilde{V}$. For other variable-density flows, this finding may not be true and prudence is called for in attempting a comparison.

5 Approach to self-preservation

The jet characteristics downstream of $x/D = 10$ are shown in Figs. 9 and 10. Again, centerline values are used to normalize the flow properties for presentation. The mean jet properties are plotted against the similarity coordinate $\eta = r/\delta_u$. In addition, the scalar half widths, δ_θ and δ_c, are also determined from the $\bar{\theta}$ and $\bar{C}$ profile plots. Based on the measured half-

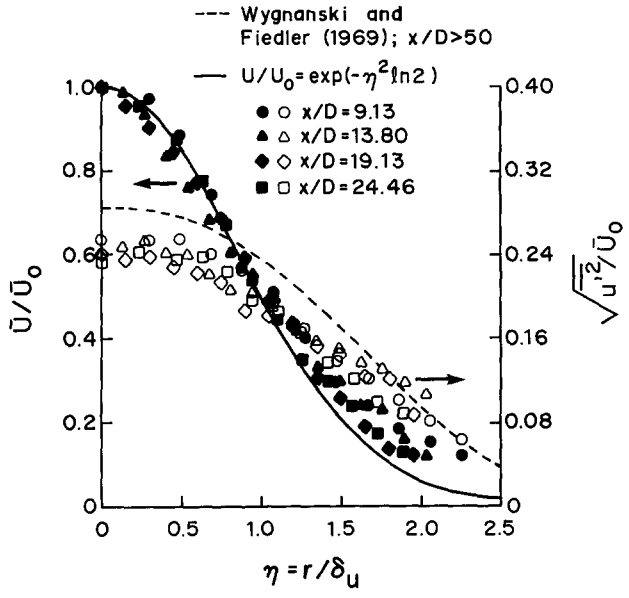

Fig. 9. Mean and rms of u across the jet in the far field

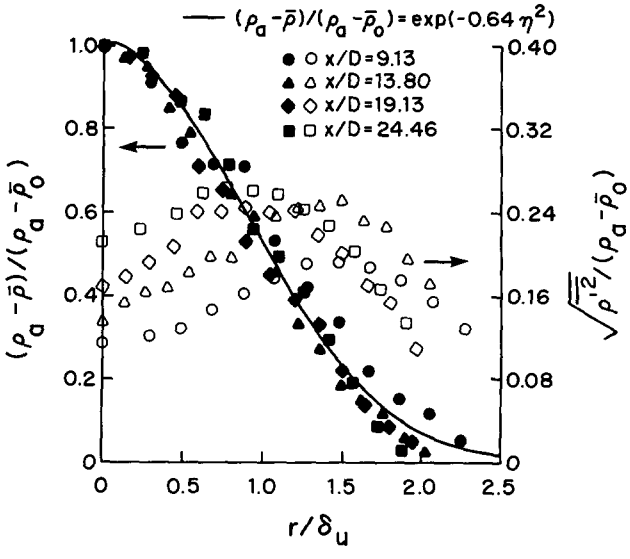

Fig. 10. Mean and rms of ϱ across the jet in the far field

widths and the analysis of So and Liu (1986), similarity distribution for $(\varrho_a-\bar{\varrho})/(\varrho_a-\bar{\varrho}_0)$ is found to be given by

$$\frac{\varrho_a-\bar{\varrho}}{\varrho_a-\bar{\varrho}_0}=\exp(-0.624\,\eta^2). \tag{9}$$

Also, the similarity distribution for $\bar{U}/\bar{U}_0$ is given by the Gaussian error-function

$$\frac{\bar{U}}{\bar{U}_0}=\exp(-\eta^2\ln 2). \tag{10}$$

These two expressions are plotted in Figs. 9 and 10 for comparison with the measured profiles. The coefficient ln 2 in (10) seems to be universal for velocity and temperature distribution in self-preserving regions of both circular and plane jets (Kotsovinos 1985; Ötügen and Namer 1988) and has been used by So and Liu (1986) to analyze binary gas jets. Their analysis gives growth and decay rates that are in excellent agreement with the measurements of Keagy and Weller (1949) and Birch et al. (1978).

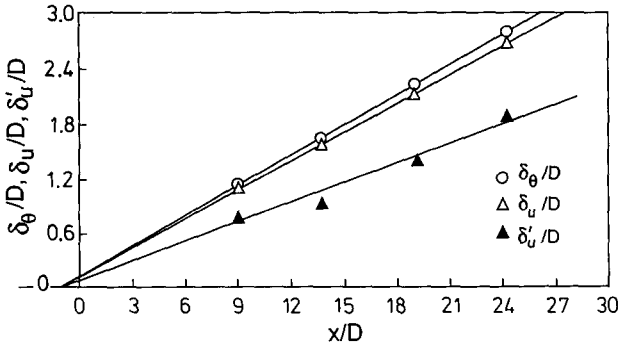

Fig. 11. Jet growth in the far field

Recently, Dowling and Dimotakis (1988) suggested that jet flow similarity could also be examined by normalizing r by $(x-x_0)$ instead of by δ_u or δ_θ. For jets with a linear growth rate, it can be shown that the similarity coordinate η is essentially equivalent to the coordinate $r/(x-x_0)$. The jet growth based on the measured δ_u or δ_θ is shown in Fig. 11. In addition, the growth of δ'_u is also plotted. It can be seen that the growth rate, whether based on δ_u, δ_θ or δ'_u, is essentially linear, thus indicating that the entrainment is jet-like and is not influenced by buoyancy for $x/D \leq 24.5$. Furthermore, the virtual origin x_0 determined by extrapolating these linear curves to zero is identical. This means that the similarity coordinate, $r/(x-x_0)$, agrees with η to within a constant. Consequently, local similarity can be examined by using a similarity coordinate of $r/(x-x_0)$, or η.

The mean velocity field is seen to approach self-preservation at $x/D=19.13$ because the measured profile at this location can be approximated very well by the Gaussian error-function. For an air jet, the measurements of Wygnanski and Fiedler (1969) showed that the turbulence field achieved self-preservation at $x/D=50$, while self-preservation of the mean velocity field was observed at $x/D=40$. The present measurements seem to show that the turbulence field has approached self-preservation at $x/D=24.46$. In order to further verify the approach to self-preservation at $x/D=24.46$ for the turbulence field, the quantity $(\overline{u'^2}/\overline{u_0'^2})^{1/2}$ is plotted against η in Fig. 12 and compared with the self-preserving measurement of Wygnanski and Fiedler (1969). The two sets of data essentially behave similarly across the jet, and strongly suggests that both the mean and turbulent velocity fields have achieved self-preservation at $x/D=24.46$.

Another point to note about the comparison in Fig. 12 is the remarkable agreement shown between the two sets of data. While the Reynolds number for the present study is 4,300, this parameter was reported to be 100,000 in the study of Wygnanski and Fiedler (1969). The result, therefore, sug-

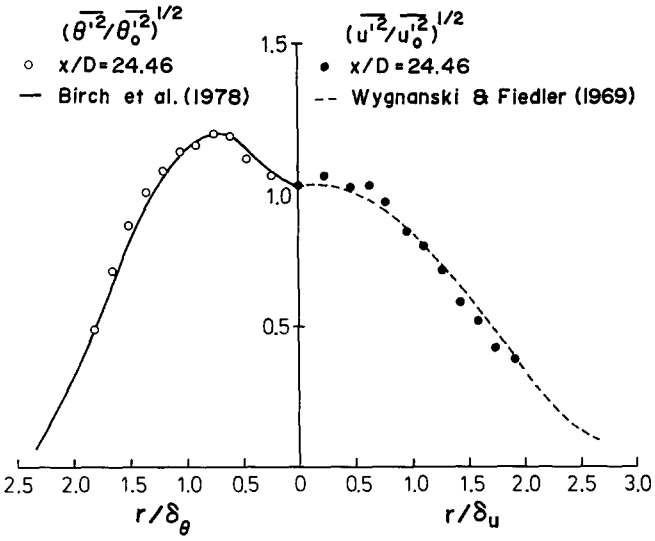

Fig. 12. A comparison of the rms of u and ϱ with other measurements

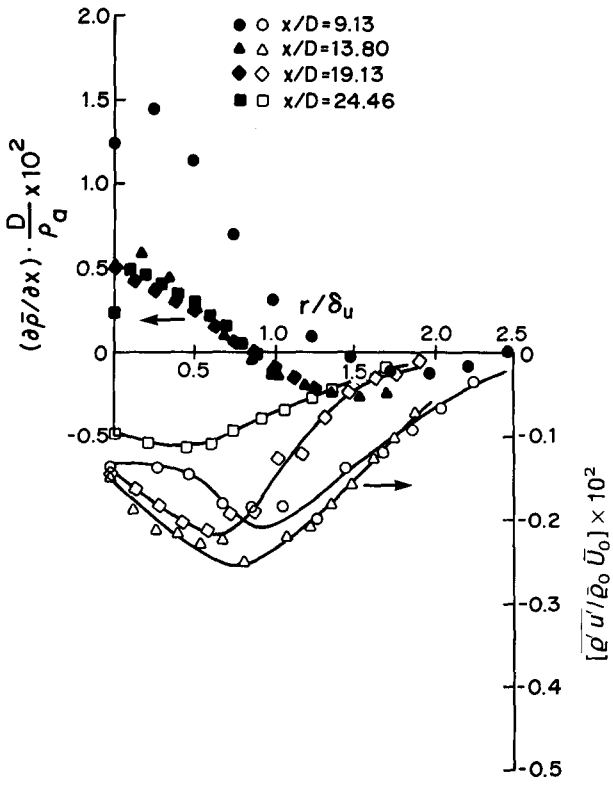

Fig. 13. Distributions of the mass flux, $\overline{\varrho' u'}$, and the mean density gradient, $\partial\bar{\varrho}/\partial x$

gests that, in the far field, once the flow reaches a self-preserving state, it is not only independent of the jet Reynolds number but is also independent of σ_1. On the other hand, for the binary gas jet investigated, self-preservation is achieved at $x/D \cong 24$. This points to a possible σ_1 effect on the development rate of the jet. However, it should be pointed out that there is a fundamental difference between the homogeneous and the variable-density jet. That is, at some axial distance downstream, the buoyancy induced momentum flux could become significant enough to modify the turbulence field and the entrainment rate. As a result, the self-preserving behavior of the variable-density jet cannot be assumed to sustain. The comparison also lends credence to the claim of Zhu et al. (1988) that the presence of the concentration probe has little or no effect on the measured velocities.

Most researchers (e.g. Birch et al. 1978; Pitts and Kashiwagi 1984) show that, when self-preservation is achieved, $\bar{\theta}/\bar{\theta}_0$ is again described by the Gaussian error-function (10) with η replaced by η_θ, and when $\overline{\theta'^2}/\overline{\theta_0'^2}$ is plotted against η_θ, the distribution becomes independent of x. This implies that the density field is also self-preserving. The plots of $(\varrho_a - \bar{\varrho})/(\varrho_a - \bar{\varrho}_0)$ versus η are shown in Fig. 10 together with the theoretical curve given by (9). It can be seen that self-preservation of the mean density field is essentially achieved at $x/D = 24.46$. However, it does not seem that the fluctuating density (or the scalar field) has accomplished self-preservation at this location. Both Birch et al. (1978) and Pitts and Kashiwagi (1984) have shown that $(\overline{\theta'^2}/\overline{\theta_0'^2})^{1/2}$ achieves self-preservation at $x/D > 20$ and that their measured distributions are essentially identical. Therefore, a further check on self-preservation can be obtained by comparing the present measurements at $x/D = 24.46$ with those of Birch et al. (1978) at $x/D = 40$ or of Pitts and Kashiwagi (1984) at $x/D = 35$. This is shown in Fig. 12. Excellent agreement is obtained between the present results and the data of Birch et al. (1978). Therefore, it can be concluded that the density or scalar field also achieves self-preservation at $x/D = 24.46$.

The remarkable agreement between the measured $\overline{\theta'^2}$ and those of Birch et al. (1978) leads to another important conclusion. Since the σ_1's for these two jets differ by about 15%, while Re is a factor of four greater for the methane jet, the close agreement again suggests that, in the jet far field, once self-preservation is achieved, the scalar field is independent of σ_1 and Re. Furthermore, the result verifies the claim that the presence of LDA seed particles in the flow does not affect the measurements of the concentration probe. It also shows that the rather simple and inexpensive laser/hot-wire technique is just as good as the more sophisticated and expensive Raman and Rayleigh scattering techniques (Birch et al. 1978; Pitts and Kashiwagi 1984). In the future, more complicated binary mixing studies can be investigated using the simple laser/hot-wire technique.

The mass flux $\overline{\varrho' u'}$ is shown together with $\partial\bar{\varrho}/\partial x$ in Fig. 13. It can be seen that $\partial\bar{\varrho}/\partial x$ and $\overline{\varrho' u'}$ are of opposite sign only for $\eta < 0.8$. In the jet outer region, $\overline{\varrho' u'}$ and $\partial\bar{\varrho}/\partial x$ are of the same sign. Consequently, (4) is not an appropriate relation for the mass flux in this region. The outer jet region is strongly intermittent and is controlled by large-scale motions. The gross, very rapid incorporation of the ambient fluid into the jet by the mechanics of the large vortices is not countered by the small scale mixing, thus leaving large portions of un-

mixed surrounding fluid in this region of the jet. In the inner jet region, by contrast, the mixing process is controlled by well developed turbulent activities. Therefore, one can conjecture that (4) holds true only in well-mixed turbulent flows. Finally, the identical behavior of $\partial\bar{\varrho}/\partial x$ at $x/D=19.13$ and 24.46, perhaps, suggests that self-preservation of the jet mean field is actually achieved at $x/D\simeq 20$.

6 Jet growth and centerline decay

The growth rates of δ_u and δ_θ are determined from Fig. 11 and listed in Table 1 for comparison with other jet data in the literature. Among the more complete jet growth and centerline decay measurements available in the literature are the experiments of Keagy and Weller (1949), Birch et al. (1978), Dyer (1979) and Pitts and Kashiwagi (1984). These data are also included for comparison in Table 1. Therefore, the data selected covers a jet-to-air density ratio range of $0.14<\sigma_1\leq 1.52$ and a Reynolds number range of $3{,}300\leq Re\leq 10^5$. The present measurements of jet growth are consistent with those reported in the literature and essentially follow the trend indicated by previous data.

In order to examine the decay characteristics properly, a third set of measurements was carried out along the jet centerline in the x/D range of $0<x/D<30$. Simultaneous measurements of ϱ and u were made and the results are used to deduce the centerline decay behavior of ϱ, u, c and θ. The results for the velocity are shown in Fig. 14, while those for c and θ are plotted in Fig. 15. In Fig. 16, the centerline decay of $\bar{\varrho}$ is given together with the behavior of $\overline{\varrho' u'}$.

The inverse decay curves can be approximated by straight lines beyond $x/D=6.0$ for u, ϱ, θ and c. However, if the straight lines are drawn through the measurements in the x/D range of $15<x/D<30$, then the slopes of these lines are as given in Table 1. Again, the determined slopes are consistent with literature data. Thring and Newby (1953) introduced the concept of an effective diameter d_ε to account for density difference between the jet and ambient fluids. If this concept is also used to represent the hyperbolic decay laws for u, ϱ, θ and c, then

$$\frac{\bar{U}_0}{U_j}=\frac{k_u\, d_\varepsilon}{x+a_u}, \tag{11}$$

$$\frac{\varrho_a-\bar{\varrho}_0}{\varrho_a}=\frac{k_\varrho\, d_\varepsilon}{x+a_\varrho}, \tag{12}$$

$$\frac{\bar{\theta}_0}{\theta_j}=\frac{k_\theta\, d_\varepsilon}{x+a_\theta}, \tag{13}$$

$$\frac{\bar{C}_0}{C_j}=\frac{k_c\, d_\varepsilon}{x+a_c}. \tag{14}$$

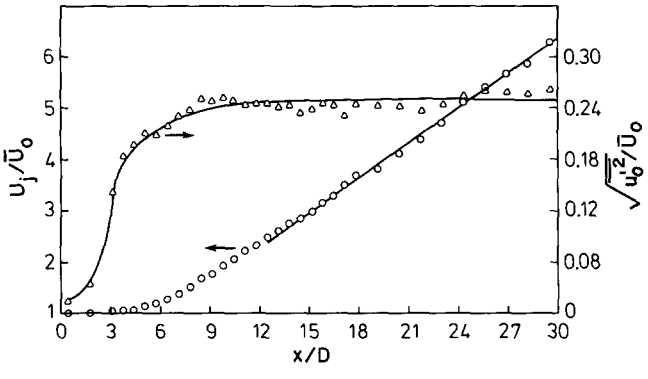

Fig. 14. Behavior of u along the jet centerline

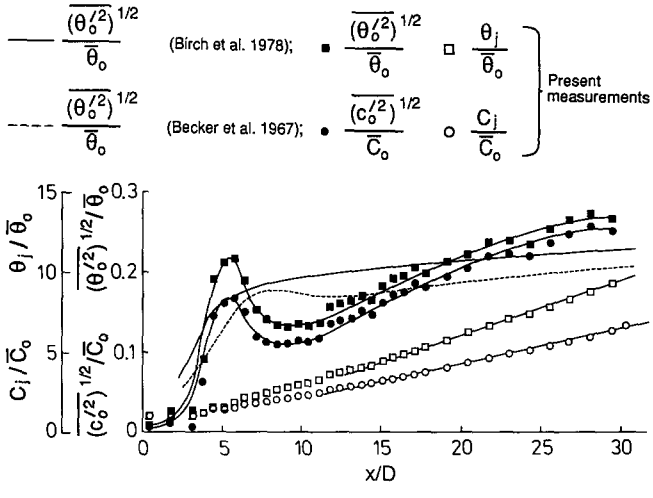

Fig. 15. Behavior of θ and c along the jet centerline

Table 1. A comparison of jet spread and decay of centerline values of different binary gas jets

Source	Jet fluid	σ_1	$\frac{U_a}{U_j}$	Rex 10^{-3}	$\frac{U_j}{\bar{U}_0}\frac{D}{x}$	$\frac{\delta_u}{x}$	$\frac{\theta_j}{\bar{\theta}_0}\frac{D}{x}$	$\frac{\delta_\theta}{x}$	$\frac{C_j}{\bar{C}_0}\frac{D}{x}$	$\frac{\delta_c}{x}$	$\frac{\varrho_a}{(\varrho_a-\bar{\varrho}_0)}\frac{D}{x}$	$\frac{\delta_\varrho}{x}$
Keagy and Weller (1949)	He	0.14	0	3.3	0.48	0.11	–	–	0.091	0.156	–	–
Birch et al. (1978)	CH_4	0.55	0	16.0	0.269	–	0.337	0.097	0.189	–	–	–
Pitts and Kashiwagi (1984)	CH_4	0.55	0.033	4.1	–	–	0.302	0.104	–	–	–	–
Present work	He/Air mixture	0.64	0	4.3	0.229	0.103	0.331	0.107	0.221	0.107	0.609	0.099
Keagy and Weller (1949)	N_2	0.96	0	25.3	0.20	0.089	–	–	0.200	0.105	–	–
Wygnanski and Fiedler (1969)	Air	1.00	0	~100.0	0.20	0.085	–	–	–	–	–	–
Keagy and Weller (1949)	CO_2	1.52	0	47.8	0.17	0.083	–	–	0.290	0.090	–	–
Dyer (1979)	C_3H_8	1.52	0.033	9.8	–	–	0.18	0.086	–	–	–	–

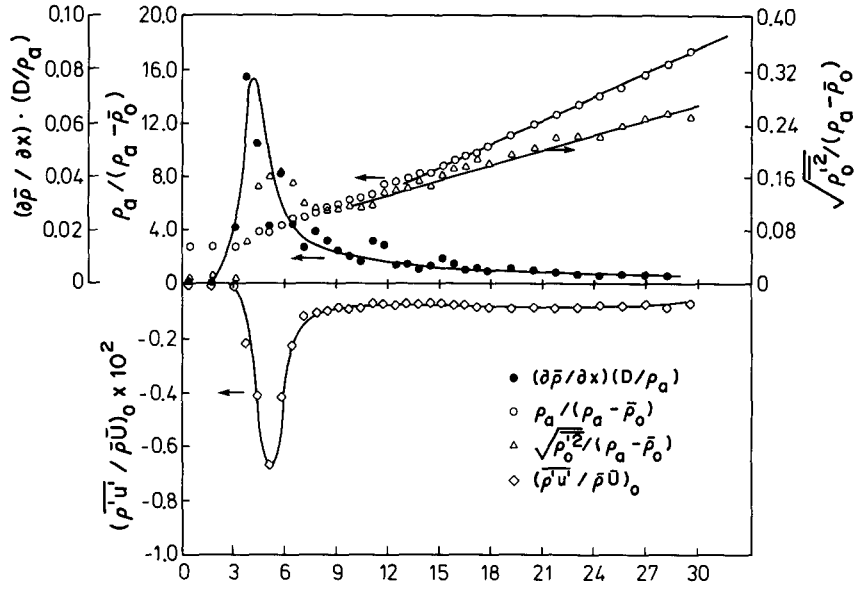

Fig. 16. Behavior of $\bar{\varrho}$ and $\overline{\varrho' u'}$ along the jet centerline

The hyperbolic decay constants thus determined are: $k_u = 5.45$, $k_\varrho = 2.05$, $k_\theta = 3.77$ and $k_c = 5.68$. If the lines as drawn in Figs. 14–16 are used to determine the constants a_c through a_u, then the following values are obtained: $a_u = -2.05\,D$, $a_\varrho = 0.74\,D$, $a_\theta = -1.54\,D$ and $a_c = -0.84\,D$. The k_u and k_θ thus determined are in agreement with those reported by Keagy and Weller (1949), Wgynanski and Fiedler (1969), Birch et al. (1978) and Pitts and Kashiwagi (1984). Therefore, these results substantiate the conclusion of So and Liu (1986) and illustrate that the concept of an effective diameter can indeed be used to account for density difference between the jet and ambient fluids.

The measurements of Birch et al. (1978) showed that the distribution of $(\overline{u_0'^2})^{1/2}/\overline{U_0}$ increases rapidly in the jet near field, but quickly tapers off to a value of ~ 0.31 in the far field. The present measurements of $(\overline{u_0'^2})^{1/2}/\overline{U_0}$ follow the same trend as Birch et al.'s data with an asymptotic value of about 0.24 reached at $x/D = 30$. On the other hand, the distribution of $(\overline{\theta_0'^2})^{1/2}$ follows a hyperbolic decay in the region $15 < x/D < 30$, similar to that observed by Birch et al. (1978), who measured a limiting value of 0.285 for the θ unmixedness at $x/D = 70$. Furthermore, their measurements showed that the local value of the fluctuation intensity is lower everywhere for concentration than for velocity; an observation that is approximately true for the present data. The present data on $(\overline{\theta_0'^2})^{1/2}$ does not show a continuous rise of unmixedness in the developing region. Instead, it shows a maximum at $x/D \simeq 6$ and a sharp drop to a minimum at $x/D \simeq 9$. Thereafter, it slowly increases to a value of about 0.27 at $x/D = 30$ (Fig. 15). This behavior is similar to that measured by Becker et al. (1967). However, the minimum value reached by their $(\overline{\theta_0'^2})^{1/2}$ distribution is significantly higher than the present measurement (Fig. 15). In general, the present data is consistent with those reported in the literature and the observed discrepancies between the different sets of data are within the differences noted in Birch et al.'s comparison of their data with other measurements.

In Fig. 16, the distribution of $(\overline{\varrho_0'^2})^{1/2}/(\varrho_a - \bar{\varrho}_0)$ in the jet far field is found to be linear rather than hyperbolic. Furthermore, the gradient diffusion relation (4) is found to be approximately valid along the jet centerline where $\overline{\varrho' u'}$ is negative. This implies that a fairly developed turbulence field prevails along the jet axis.

Conclusions

As a result of this study, the following conclusions can be drawn.

The simple laser/hot-wire technique proves to be a viable technique for the study of mass and momentum transfer in binary gas jets. The turbulent statistics thus measured provide accuracy comparable to those obtained from Raman/LDA and Rayleigh/LDA techniques.

The binary gas jet studied achieved self-preservation at $x/D \simeq 24$ for both the velocity and density fields.

In the central portion of the jet, where the turbulence field is fairly developed, the gradient diffusion assumption for the mass flux $\overline{\varrho' u'}$ seems to be valid even though the diffusion coefficient may be varying across the jet. Near the jet edge, where the flow is intermittent, the gradient diffusion assumption for $\overline{\varrho' u'}$ is not valid. This is true for both the near and far fields of the jet.

Even though the gradient diffusion assumption is not valid for $\overline{\varrho' u'}$ in the jet outer region, it is appropriate for the mass flux $\overline{\varrho' v'}$ and the turbulent shear stress $\bar{\varrho}\,\overline{u' v'}$.

In the jet near field, the mass fluxes are found to be of the same order of magnitude as the momentum fluxes. Consequently, they cannot be neglected when compared to the momentum flux terms in the Reynolds-averaged governing

equations. However, the mass flux terms decrease rapidly and become less significant in the jet far field.

The triple correlation terms $\overline{\varrho' u'^2}$ and $\overline{\varrho' v'^2}$ are at least one order of magnitude smaller than the momentum flux terms. Hence, their neglect in the jet equations is justified.

For the binary gas jet investigated, the ratio of the Favre-averaged to Reynolds-averaged axial velocity is approximately one across the jet. This suggests that a direct comparison of the calculations based on a Favre-averaged formulation of the governing equations with measurements is legitimate. However, the question of how to model the Favre-averaged flux terms still remains.

Jet growth is linear, with the growth rate for the scalar field slightly larger than that of the velocity field.

The virtual origin of the jet, determined from either δ_u, δ'_u or δ_θ, is the same. This, together with the linear growth rates, implies that the similarity coordinates η and $r/(x-x_0)$ agree with each other to within a constant.

Centerline properties follow hyperbolic decay laws. The hyperbolic decay constants thus determined are in agreement with those reported in the literature and lend credibility to the concept of an effective diameter used to account for density difference between jet and ambient fluids.

Acknowledgements

This research was sponsored by Naval Weapons Center, China Lake, CA 93555, under contract no. N60530-85-C-9001. Partial support was also received from David Taylor Research and Development Center, Annapolis, MD 21402, under contract no. N00167-86-K-0075.

References

Antonia, R. A.; Prabhu, A.; Stephenson, S. E. 1975: Conditionally sampled measurements in a heated turbulent jet. J. Fluid Mech. 72, 455–480

Batt, R. G. 1977: Turbulent mixing of passive and chemically reacting species in a low-speed shear layer. J. Fluid Mech. 82, 53–95

Becker, H. A.; Hottel, H. C.; Williams, G. C. 1967: The nozzle fluid concentration field of the round turbulent free jet. J. Fluid Mech. 30, 285–303

Bilger, R. W. 1976: Turbulent jet diffusion flames. Prog. Energy Combust. Sci. 1, 87–109

Birch, A. D.; Brown, D. R.; Dodson, G. M.; Thomas, J. R. 1978: The turbulent concentration field of a methane jet. J. Fluid Mech. 88, 431–449

Brown, G. L.; Roshko, A. 1974: On density effects and large structure in turbulent mixing layers. J. Fluid Mech. 64, 775–816

Chevray, R.; Tutu, N. K. 1978: Intermittancy and preferential transport of heat in a round jet. J. Fluid Mech. 88, 133–160

Dibble, R. W.; Kollmann, W.; Schefer, R. W. 1984: Conserved scalar fluxes measured in a turbulent nonpremixed flame by combined laser Doppler velocimetry and laser Raman scattering. Combust. Flame 55, 307–321

Dowling, D. R.; Dimotakis, P. E. 1988: On mixing and structure of the concentration field of turbulent jets. AIAA 88-2611-CP Paper

Driscoll, J. F.; Schefer, R. W.; Dibble, R. W. 1982: Mass fluxes $\overline{\varrho' u'}$ and $\overline{\varrho' v'}$ measured in a turbulent nonpremixed flame. In: Proc. 19th Int. Symp. Combust. pp. 477–485. The Combustion Institution

Dyer, T. M. 1979: Rayleigh scattering measurements of time-resolved concentration in a turbulent propane jet. AIAA J. 17, 912–914

Ferri, A.; Libby, P. A.; Zakkay, V. 1964: Theoretical and experimental investigation of supersonic combustion. In: Proc. 3rd Congress Int. Council Aeronaut. Sci. pp. 1089–1155. Baltimore/MD: Spartan Books

Fujii, S.; Gomi, M.; Eguchi, K. 1983: A remote laser-probe system for velocity and temperature measurements. J. Fluids Eng. 105, 128–133

Fujii, S.; Gomi, M.; Eguchi, K.; Yamaguchi, S.; Jin, L. 1984: Time resolved LDV and CARS measurements in a premixed reacting flow. Combust. Sci. Technol. 36, 211–226

Goss, L. P.; Trump, D. D.; Roquemore, W. M. 1988: Combined CARS/LDA instrument for simultaneous temperature and velocity measurements. Exp. Fluids 6, 189–198

Gouldin, F. C.; Schefer, R. W.; Johnson, S. C.; Kollmann, W. 1986: Nonreacting turbulent mixing flows. Prog. Energy Combust. Sci. 12, 257–303

Keagy, W. R.; Weller, A. E. 1949: A study of freely expanding inhomogeneous jets. pp. 89–98. Stanford/CA: Stanford University

Kotsovinos, N. E. 1985: Temperature measurements in a turbulent round plume. Int. J. Heat Mass Transfer 28, 771–777

Libby, P. A. 1962: Theoretical analysis of turbulent mixing of reactive gases with application to supersonic combustion of hydrogen. ARS J. 32, 388–396

Logan, S. E. 1972: A laser velocimeter for Reynolds stress and other turbulence measurements. AIAA J. 10, 933–935

Moss, J. B. 1980: Simultaneous measurements of concentration and velocity in an open turbulent flame. Combust. Sci. Technol. 22, 119–129

Ötügen, M. V.; Namer, I. 1988: Rayleigh scattering temperature measurements in a plane turbulent air jet at moderate Reynolds numbers. Exp. Fluids 6, 461–466

Pitts, W. M.; Kashiwagi, T. 1984: The application of laser-induced rayleigh light scattering to the study of turbulent mixing. J. Fluid Mech. 141, 391–429

Pitts, W. M.; McCaffrey, B. J.; Kashiwagi, T. 1983: A new diagnostic technique for simultaneous, time-resolved measurements of concentration and velocity in simple turbulent flow systems. Presented at the 4th Symp. Turbulent Shear Flows, Karlsruhe, W. Germany, September 12–14

So, R. M. C.; Ahmed, S. A. 1987: Helium jets discharging normally into a swirling air flow. Exp. Fluids 5, 255–262

So, R. M. C.; Liu, T. M. 1986: On self-preserving, variable-density turbulent free jets. Z. Angew. Math. Phys. 37, 538–558

So, R. M. C.; Yu, M. H.; Ötügen, M. V.; Zhu, J. Y. 1987: Rotation effects on inhomogeneous mixing in axisymmetric sudden-expansion flows. Int. J. Heat Mass Transfer 30, 2411–2421

Stanford, R. A.; Libby, P. A. 1974: Further applications of hot-wire anemometry to turbulence measurements in helium – air mixtures. Phys. Fluids 17, 1353–1361

Stevenson, W. H.; Thompson, H. D.; Roesder, T. C. 1982: Direct measurement of laser velocimeter bias errors in a turbulent flow. AIAA J. 20, 1720–1723

Thring, M. W.; Newby, M. P. 1953: Combustion length of enclosed turbulent jet flames. In: Proc. 4th Int. Symp. Combust. pp 789–796. The Combustion Institution

Way, J.; Libby, P. A. 1970: Hot-wire probes for measuring velocity and concentration in helium-air mixtures. AIAA J. 8, 976–978

Wygnanski, I.; Fiedler, H. 1969: Some measurements in the self-preserving jet. J. Fluid Mech 38, 577–612

Zhu, J. Y.; So, R. M. C.; Ötügen, M. V. 1988: Turbulent mass flux measurements using a laser/hot-wire technique. Int. J. Heat Mass Transfer 31, 819–829

Zhu, J. Y.; So, R. M. C.; Ötügen, M. V. 1989: Mass transfer in a binary gas jet. AIAA J. 27, 1132–1135

Received December 18, 1989